Archives of Microbiology (2023) 205:250
https://doi.org/10.1007/s00203-023-03591-z

ORIGINAL PAPER

Leveraging molecular docking to understand Congo red degradation by *Staphylococcus caprae* MB400

Zarrin Basharat[1] · Sehrish Asghar[2] · Azra Yasmin[3]

Received: 21 February 2023 / Revised: 11 April 2023 / Accepted: 18 May 2023 / Published online: 27 May 2023

Abstract

Congo red (CR) is a genotoxic, sulphonated azo dye and poses significant pollution problem. We hereby report its degradation by *Staphylococcus caprae* MB400. The bacterium initially propagated as a suspected contaminant upon CR dye supplemented nutrient agar plates, forming zones of clearance around its growth area. The bacterium was purified, gram stained and identified as *Staphylococcus caprae* via 16S rRNA gene sequencing. Dye decolourization was analysed in liquid culture, and Fourier-transform infrared spectroscopy (FTIR) was conducted for analysis of degraded product/metabolites. A decolourization of ~ 96.0% at 100 µg/ml concentration and pH 7 after 24 h of incubation was observed. Structure of the azoreductase enzyme, responsible for breakage of the bond in the dye and ultimately decolourization, was predicted, and molecular docking was harnessed for understanding the mechanism behind the reduction of azo bond (–N=N–) and conversion to metabolites. Our analysis revealed 12 residues critical for structural interaction of the azoreductase enzyme with this dye. Among these, protein backbone region surrounding four residues, i.e. Lys65, Phe122, Ile166 and Phe169, showed major displacement changes, upon binding with the dye. However, overall the conformational changes were not large.

Keywords Congo red · Azoreductase · Bioremediation · Molecular docking · Bioinformatics

Introduction

Azo dyes are a diverse group of synthetic colorants, widely used in various industries (Guo et al. 2020). The global concerns about the potential hazards of azo dyes have risen over past few years, as they are xenobiotic and recalcitrant in nature (Fernando et al. 2019; Picho-Chillan et al. 2019). Disposal of these dyes into the environment causes serious damage, since they may significantly affect the photosynthetic activity of hydrophytes by reducing light penetration and also they may also be toxic to aquatic organisms due to their breakdown products (Hernández-Zamora and Martínez-Jerónimo 2019). These dyes may alter pH of environment, increase biochemical oxygen demand and chemical oxygen demand and give deep coloration to water bodies and/or surrounding environments in which they are discharged (Yadav et al. 2013; Katal et al. 2014; Dinçer 2020). The removal of dyes from industrial waste is necessary, from health and hygiene point of view and for environmental protection, before their entrance and potential toxicity into the water bodies.

Removal of coloured dyes from industrial effluents can be achieved by different conventional methods such as ozonation, photooxidation, electrocoagulation, adsorption, activated carbon, froth flotation, reverse osmosis and membrane filtration. These physiochemical techniques are not economical and also are less efficient in terms of restricted applicability and may generate waste which is difficult to dispose (Chen et al. 1999; Singh and Arora 2011; Shah 2019). Methods that do not generate any waste like

Communicated by Yusuf Akhter.

✉ Zarrin Basharat
zarrin.iiui@gmail.com

✉ Azra Yasmin
azra.yasmin@fjwu.edu.pk

Sehrish Asghar
sehr.asghar@gmail.com

[1] Alpha Genomics (Private) Limited, Islamabad 45710, Pakistan

[2] Environmental Science Program, College of Natural Resources, University of Idaho, Moscow, ID 83843, USA

[3] Microbiology and Biotechnology Research Lab, Department of Biotechnology, Fatima Jinnah Women University, Rawalpindi 46000, Pakistan

advanced oxidation products and membrane filtrations are not cost-effective and linked with more energy utilization (Pandey et al. 2007; Yagub et al. 2014). Biological treatment methods, through which the removal of dyes from polluted environment can be achieved for decolourization of dyes, are considered more feasible and efficient. Various microorganisms and their enzymes azoreductases and oxidases capable of decolorizing azo dyes have been isolated and characterized (Suzuki et al. 2001; Blümel et al. 2002; Koyani et al. 2013; Oturkar et al. 2013; Sarkar et al. 2020).

Microbes are economically feasible source of remediation of azo dyes. The decolourization of azo dyes with bacteria can be undertaken in wide range of environments, by different groups of bacteria (Saratale et al. 2013; Naseer et al. 2016; Eskandari et al. 2019). To understand the bioremediation interactions, computational docking has also been employed for observing interaction between various enzymes and azo dyes (Basharat et al. 2017; Srinivasan and Sadasivam 2018). The present study aimed to investigate a bacterium isolated as a contaminant, later identified as *Staphylococcus caprae* for decolourization of CR, a sulphonated azo dye, under various environmental conditions, i.e. concentration of dye, pH, temperature and static or agitating conditions of incubation. This was followed by database mining and in silico analysis of azoreductase enzyme responsible for this degradation phenomenon.

Materials and methods

Initial characterization

The bacterium propagating as contaminant on dye supplemented agar plate was named MB400, isolated and purified. Physical and biochemical characterization of parameters like colony morphology, gram's staining, growth on Eosin Methylene Blue (EMB) agar, MacConkey's agar, etc., was carried out. DNA extraction was done through phenol chloroform method (Wilson 1987; Cheng and Jiang 2006), followed by PCR amplification of the 16S rRNA gene using universal set of primers. The product was sequenced by Macrogen (Korea). Obtained FASTA sequence file was subjected to BLAST analysis and alignment with significant hits (of rRNA gene sequences) in the NCBI database to reveal genus and species of the bacterium under consideration. The bacterium was identified as *Staphylococcus caprae*. Similar 16S rRNA gene sequences were derived by BLAST and aligned along with 16S rRNA sequence of *Bacillus rhizoplanae* strain JJ-63 as an out-group (Accession ID: NR_181926.1). Phylogenetic analysis was conducted using MEGA-X software (Kumar et al. 2018). Initial tree(s) for the heuristic search were obtained automatically by applying Neighbour-Join and BioNJ algorithms to a matrix of pairwise distances estimated using the Jukes–Cantor model (Erickson 2010), and then selecting the topology with superior log likelihood value.

Study of decolourization activity

Nutrient agar was obtained from Merck, and CR (IUPAC name: disodium 4-amino-3-[4-[4-(1-amino-4-sulfonatonaphthalen-2-yl)diazenylphenyl]phenyl]diazenyl-naphthalene-1-sulfonate) was purchased from Sigma-Aldrich. All experiments were performed in sterile conditions. Decolourization experiments were carried out on both solid agar slants and in liquid nutrient broth medium. 100 ml flasks were used for liquid culturing with varied amounts of dye concentration. Incubation at different temperatures (25, 37, 40 °C), pH (6, 7, 8) and in static as well as shaking condition was done for 24 and 48 h. This was followed by centrifugation at 3000 rpm for 10 min and determination of decolourization activity by spectrophotometer (PG Instruments) at an absorbance of 498 nm. The nutrient broth was taken as blank and broth with dye as control. Decolourization was calculated as described previously (Aftab et al. 2011).

FTIR analysis was carried out to determine fate of dye inside cell mass. The cell mass of control and experimental samples (settled at the base of tubes after centrifugation) was dried in desiccator for 72 h, mixed with KBr in 1:20 ratio separately, ground and pressed with hydraulic presser to obtain IR- transparent pellets. The absorbance FTIR spectra were collected (using FTIR-8400, SCHMIDZU) within a scanning range of 4000–250 cm^{-1}. The FTIR was calibrated for background signal scanning with a control sample of pure KBr pellet, and then, the experimental samples were scanned. The FTIR spectrum of control was finally compared with spectra of sample to observe changes in their IR peaks.

Bioinformatic analysis

The azoreductase family comprises an array of enzymes with varied structure and functional properties. Evolution has also impacted the sequence conservation along with selection pressure and mutations. To study the details of this, enzyme sequences of *Staphylococcus caprae* azoreductase, responsible for dye degradation, were obtained from the NCBI database with accession number WP_002444591.1 (208 amino acid) and WP_002441143.1 (188 amino acid). These paralogs were subjected to alignment with CLUSTALW and synteny analysis with other *Staphylococcus* spp. Subcellular localization was predicted using PSORTb server (https://www.psort.org/psortb/; accessed 10 April, 2023) (Yu et al. 2010). Structure modelling was done through SWISS-Model (Kiefer et al. 2009) using indigo reductase from *Bacillus smithii*-type strain DSM 4216 (PDB ID: 6JXN) as template.

Sequence identity was 63.94, and coverage was 100%. Structure was refined using Molecular Operating Environment v2019.0102 (MOE). 3D protonation was done in a neutral environment. System was optimized, with ASN/GLN/HIS flip allowed. A force constant of 5000 was used for tethering the receptor, with a buffer constant of 0.25, and structure was refined to 0.1 kcal/mol/A. The dye structure was obtained from PubChem and converted to 3D conformation. It was then prepared for docking after a wash at pH:7 and dominant protonation in MOE. Docking was done with triangle placement matcher method (return poses = 1000), receptor was kept rigid, and rescoring was done with London dG (30 poses) and GBVI/WSA dG (5 poses). Top conformer with least S value was selected for further processing. Docked protein MM/GBSA energy was calculated using SVL script. The parameters were: salt: NaCl, concentration: 0.1 M, temperature = 300 K, interior dielectric = 1 and exterior dielectric = 80. Oral and *Tetrahymena pyriformis* toxicity was predicted using admetSAR 2.0 (Yang et al. 2019). Molecular dynamics (MD) simulation study was conducted for 100 ns using Desmond (Schrodinger Inc.). The system was prepared by solvating and neutralizing the complex, followed by energy minimization (Basharat et al. 2023). Finally, various analyses were performed on the trajectory in Bio3D package of R, to understand the behaviour of the system. Overlap between CR bound and unbound azoreductase protein was also done by normal mode analysis (Suhre and Sanejouand 2004).

Results

Staphylococcus caprae was initially isolated from goats (Devriese* et al. 1983; Vandenesch et al. 1995) and later from humans, mostly immunocompromised (Kanda et al. 1991; d'Ersu et al. 2016). It is difficult to isolate it from environment, and according to the authors knowledge, this is the first report where we report its propagation as contaminant in laboratory. We characterized the bacterium and then subjected to detailed wet and dry laboratory analysis for dissection of CR degradation mechanism. The 16S rRNA gene sequence of this strain has been deposited in NCBI, with the accession number KP723540.1. Phylogenetic tree of closely related sequences is shown in Figure 1.

Physicochemical characteristics of bacterium

Whitish colonies were observed for isolated *Staphylococcus caprae* MB400 strain with naked eye and brown under the microscope. Texture was moist and creamy, while gram staining was positive. Growth of strain on various media revealed that it was incapable of utilizing lactose (as did not show growth on agar) as well as lacked an ability to ferment

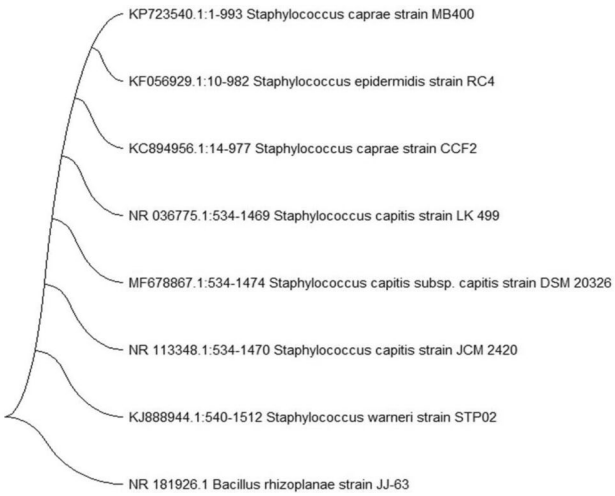

Fig. 1 Phylogenetic tree was inferred by using the maximum likelihood method. The tree is drawn to scale, with branch lengths measured in the number of substitutions per site. This analysis involved 7 nucleotide sequences from NCBI, based on BLAST similarity and one out-group (*Bacillus* sp.). Codon positions included were first, second, third and noncoding. There were a total of 1542 positions in the final dataset, and the final tree had a log likelihood of − 2646.24

(as did not show growth on MacConkey's agar). It was also coagulase negative.

Dye decolourization and degradation analysis

The bacterium was capable of growth and degradation of dye tested up to 400 µg/ml. Optimum degradation was achieved at pH 7 and temperature 40 °C (Table 1) in shaking condition (150 rpm/min). Decolourization was also tested under static condition at 37 °C and pH 7. Static conditions were found suitable for *Staphylococcus caprae* MB400 as it showed 97.67% and 98.33% decolourization after 24 and 48 hours of incubation, respectively.

More decolourization was observed at static condition which means aeration had little role in stimulating bacterium, and it was more prone to anaerobic mode of action. This also means that adsorption of dyes to cell surface for enhanced dye degradation was of little importance and degradation through absorption and enzymatic dye processing or release of enzymes into the medium was more prospective.

FTIR spectrum of CR control showed specific peaks in fingerprint region for unsubstituted and multi-substituted naphthalene or benzene rings. This was supported by the peaks (559 cm^{-1} for C–C bending vibrations), 680 cm^{-1} (for C–H stretching vibrations for disubstituted aromatic compound), 875 cm^{-1} (for p-disubstituted ring vibrations), 1093 cm^{-1} (for S=O stretching vibrations of sulfonic acid), 1261 cm^{-1} (for C–N bending vibrations), 1400 cm^{-1} (for aromatic C=C stretching vibrations), 1647 cm^{-1} (for N=N

Table 1 Percentage decolourization of CR by *Staphylococcus caprae* MB400 over a range of temperature and pH after 24 h (86,400 s) and 48 h (172,800 s) time period

Time scale (hr)	pH			Temperature (°C)		
	6	7	8	25	37	40
24	92.48	96.01	94.07	47	96.1	96
48	93.01	92.03	92.65	92.7	92.3	94.4

stretching vibrations), 3132 cm^{-1} (for O–H stretching vibrations).

The FTIR spectrum of *Staphylococcus caprae* MB400, after 24 hours of decolourization, showed peaks at 3103.5 cm^{-1} (C–H in aromatic compounds), 2850.88 cm^{-1} (CH stretching in alkanes), 1662.69 cm^{-1} (C=O stretching vibrations in amide), 1394.58 cm^{-1} (CH3 symmetrical vibrations in aromatic compounds), 1261.44 cm^{-1} (aromatic C–N stretching), 1093.67 cm^{-1} (C–N stretching of aliphatic amine), 1022.31 cm^{-1} (C–N stretching in alkyl amine), 875.71 cm^{-1} (CH out of plane deformation in meta-disubstituted aromatic compounds), 800.49 cm^{-1} (CH out of plane vibrations for para-disubstituted aromatic compounds), 561.30 cm^{-1} (C-Br stretching in alky bromide). The spectrum taken after 48 hours of decolourization showed peaks at 1394 cm^{-1} (CH3 symmetrical vibrations in aromatic compounds), 1261 cm^{-1} (aromatic C–N stretching), 1095.60 cm^{-1} (C-N stretching of aliphatic amine), 1024.24 cm^{-1} (C–N stretching in alkyl amine), 875.71 cm^{-1} (CH out of plane deformation in meta-disubstituted aromatic compounds), 802.41 cm^{-1} (CH out of plane vibrations for para-disubstituted aromatic compounds), 561 cm^{-1} (C-Br stretching in alky bromide). The spectrum of supernatant had peaks at 1647.26 cm^{-1} (CN bending vibrations of primary amine), 1400.37 cm^{-1} (CH3 symmetrical vibrations in aromatic compounds), 1261.49 cm^{-1} (aromatic C-N stretching), 1180.60 cm^{-1} (C–N stretching in alkyl amine), 1068.60 cm^{-1} (C–N stretching aliphatic amines), 875.71 cm^{-1} (CH out of plane deformation in meta-disubstituted aromatic compounds), 798.56 cm^{-1} (CH out of plane vibrations for para disubstituted aromatic compounds), 599.88 cm^{-1} (C–Br stretching in alky bromide) (Supplementary Figure 1).

Conservation and structural prediction

Alignment of sequences showed very little conservation (Figure 2). Synteny analysis showed conservation of gene apparatus in 71 *Staphylococcus* species, ranging from 83% in *Staphylococcus haemolyticus* to 19% in *Staphylococcus*

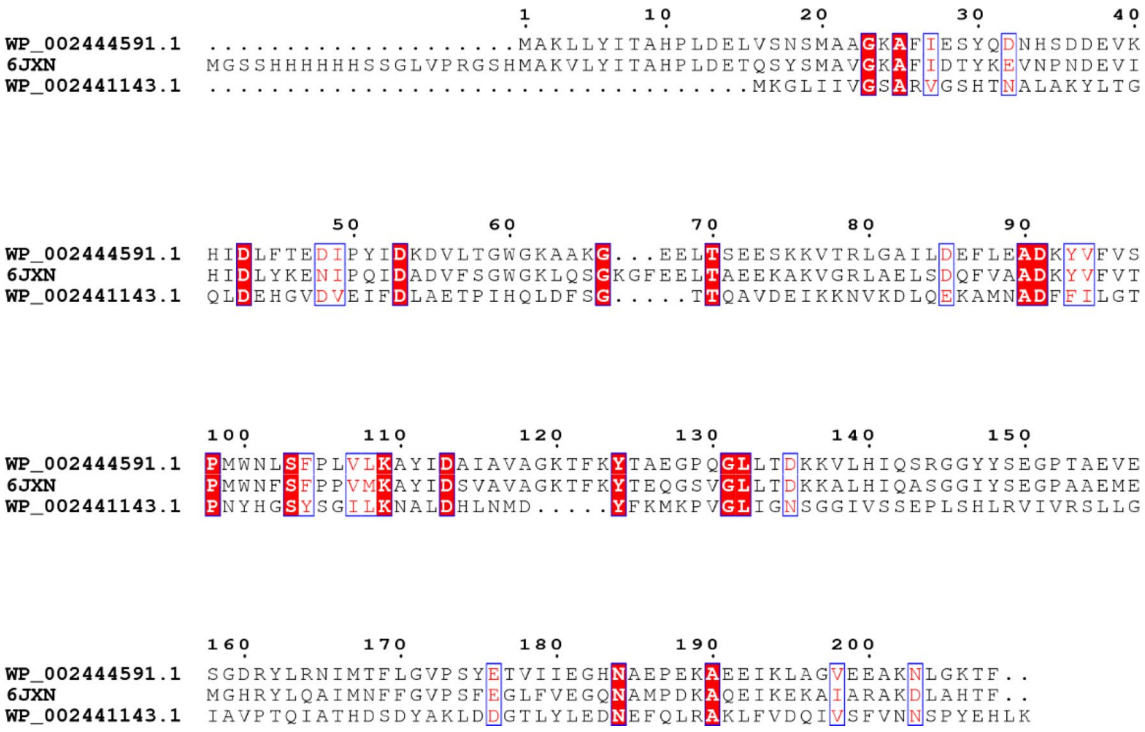

Fig. 2 Aligned residues of both isoforms of azoreductase from *Staphylococcus caprae* and the sequence of indigo reductase from *Bacillus* sp., used for modelling the final structure of longest isoform. Red regions show conservation

xylosus. Capsule synthesis genes and beta-lactamase genes were found in immediate vicinity of azoreductase. No conservation of azoreductase genes was observed for 86 *Staphylococcus* species. Azoreductase sequence domain with accession PRK00170, spanning amino acid region 1-207 with E value of $4.82e^{-107}$, was observed for first paralog, while SsuE domain (for FMN reductase) from 1 to 188 amino acid with an E value of $1.45e^{-47}$ was obtained for second paralog.

We predicted the 3D structure of longer paralog (Figure 3A), i.e. with 208 amino acids, based on this approach using a template of *Bacillus smithii* indigo reductase. Indigo reductase has a role in in the fermentation process responsible for aidate (indigo dyeing). Total 388 templates were found, and the homo dimeric 231 amino acid long template (PDB ID: 6JXN) with most similarity was used for structure building. Modelled structure (Figure 3A) had a global model quality estimate of 0.83 and Qmean of -1.23. Global quality score is between the range 0 and 1, and higher number means better model. Qmean is a composite quality score, with value below − 4 indicative of bad models. Our protein had better scores, showing a good quality. Ramachandran plot (Figure 3B) depicted 94.66% residues in most favoured regions. Only 0.73% residues were outliers.

Docking analysis

Docking can provide valuable insights into the binding affinity and specificity of a ligand. For this purpose, first property analysis and structure preparation of both enzyme and dye were done. The topological surface area of CR was 232.64 $Å^2$ with octanol water partition coefficient of − 0.05. Molecular weight of the compound was 696.68 g/mol. An acute oral toxicity of 3.626 kg/mol and pIGC50 of 1.067 ug/L for Tetrahymena pyriformis was predicted. Total 432 conformations were obtained for the enzyme binding, using rotate bond, and 299 site points were recorded with triangle matcher method. 994 non-duplicate binding poses were obtained, and refined and top complex with least S value of − 6.63 was selected for interaction analysis. Three residues (Table 2) made bonded interactions, while non-bonded interactions were observed for other nine residues (Figure 4).

Six interactions were with polar (Lys54, Thr58, Gly61, Lys62, Lys65 and Tyr124) and six with greasy residues (Leu57, Trp60, Ala116, Phe122, Ile166 and Phe169). No interactions with acidic residues were observed. Thr58 made an arene-H bond interaction and Lys65 donated electrons at two positions, while Thr124 at one position of the sulphonated region of the dye. MM/PBSA energy of CR was − 55.427, while after binding with enzyme was − 17.627.

MD simulation analysis

MD simulation can be particularly useful for validating and complementing the docking analysis. Docking is limited to predicting the static binding mode, but MD simulations can provide information about the dynamic behaviour of the complex and the binding stability over time. By comparing the results of docking with MD simulations, one can validate the predicted binding mode and determine if it is stable over time. This can help to improve the accuracy of docking predictions and provide a more detailed understanding of the molecular interactions involved in ligand–receptor binding.

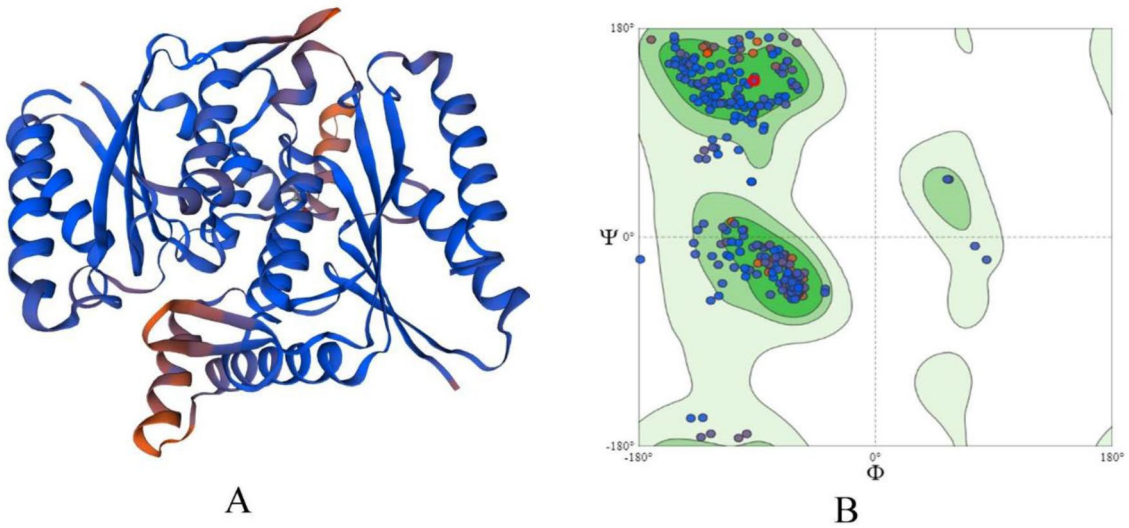

Fig. 3 **A** 3D structure of the azoreductase of *Staphylococcus caprae*. Structure is depicting both chains in the figure. **B** Ramachandran plot analysis of the structure showing majority residues in favoured region. Only two outliers, i.e. ILE115 and PRO129, were observed. 6 C-beta deviations and 1 twisted non-proline were observed

Table 2 Bonded interactions of CR with *Staphylococcus caprae* azoreductase at atomic scale

Ligand atom	Ligand atom position	Receptor atom	Residue	Position	Interaction	Distance	Energy (kcal/mol)
O	3	OH	TYR	124	H-acceptor	3.36	− 1.0
O	4	NZ	LYS	65	H-acceptor	3.01	− 3.1
O	7	NZ	LYS	65	H-acceptor	3.04	− 4.8
O	4	NZ	LYS	65	Ionic	3.01	− 4.4
O	7	NZ	LYS	65	Ionic	3.04	− 4.2
6-ring		CA	THR	58	pi-H	3.68	− 0.6

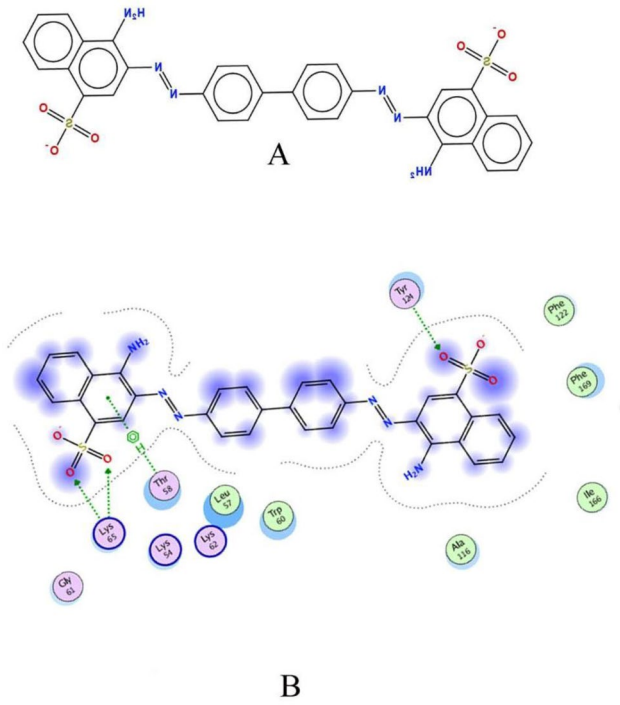

Fig. 4 **A** 2D structure of the CR dye. **B** 2D interaction plot of the receptor-dye plot. Dye exposure area to solvent residues is shown in blue, while proximity contour is shown by dotted line. Arrows indicate direction of electron transfer

Simulation results revealed stable binding, with RMSD values not exceeding 3 Å for azoreductase (Fig. 5A). Residues near position 60–70 (helical and loop region), around position 125 (loop region) and 150 (loop regions), showed flexibility (Fig. 5B). Principal component analysis (PCA) of the simulation trajectory revealed higher eigenvalues for PC1, followed by lower values for PC2 and PC3 (Fig. 5C, D and E). The fact that PC1 had the highest eigenvalue means that it captures the most important and dominant motion or conformational change in the system. PC2 and PC3 captured smaller, more subtle motions or changes that occur during the simulation and were less important in explaining the overall variance in the data. However, a change of 35% does not depict very large change (Fig. 5F). This is evident from normal mode analysis as well (Fig. 6A). Overlaying the various frames of trajectory at intervals of 20 ns revealed that the CR was undergoing change in position with reference to azoreductase but not too much (Fig. 6B). The RMSD of trajectory frames with reference to complex structures complements this finding in detail (Fig. 6C). The results indicate that the system is undergoing conformational changes at small scale.

A normalized mean square displacement <R2> of all C-alpha atoms in the protein bound and unbound with CR showed a B-factor correlation of − 0.805 for C-alpha atoms for 100 normal modes. Initial two and last two modes were analysed to see the deviation. In all modes (Figure 6A), major displacement was observed around atomic region 932-1116.

This is the region linked with residues Trp60 to Glu73, and out of these 13 residue regions, four were making interactions with the CR dye. The highest displacement was observed near Lys65, i.e. at Gly66. Lys65 is involved in direct interaction with dye, and hence, the region nearby underwent conformational change as well as c-alpha displacement. Other displacements were observed at around atom number 1911-1918 (linked with residue Phe122 and Lys123) and atom number 2383-2949 (linked with several residues, including two binding residues Ile166 and Phe169). Phe122 is also making an interaction with the ligand, hence, the displacement. This confirms our analysis that binding perturbed the regions where an interaction was occurring.

Discussion

This is a distinctive study making use of an environmental bacterium to study azoic dye degradation and its *in silico* aspects. The bacterium showed good biodegradation as evident from FTIR analysis. Membrane bound azoreductase enzymes have the ability to reduce non-sulphonated azo dyes as they can diffuse through the bacterial cell membrane (Sarkar et al. 2017) and azoic dyes comprising sulphonate groups and higher molecular weights are not likely

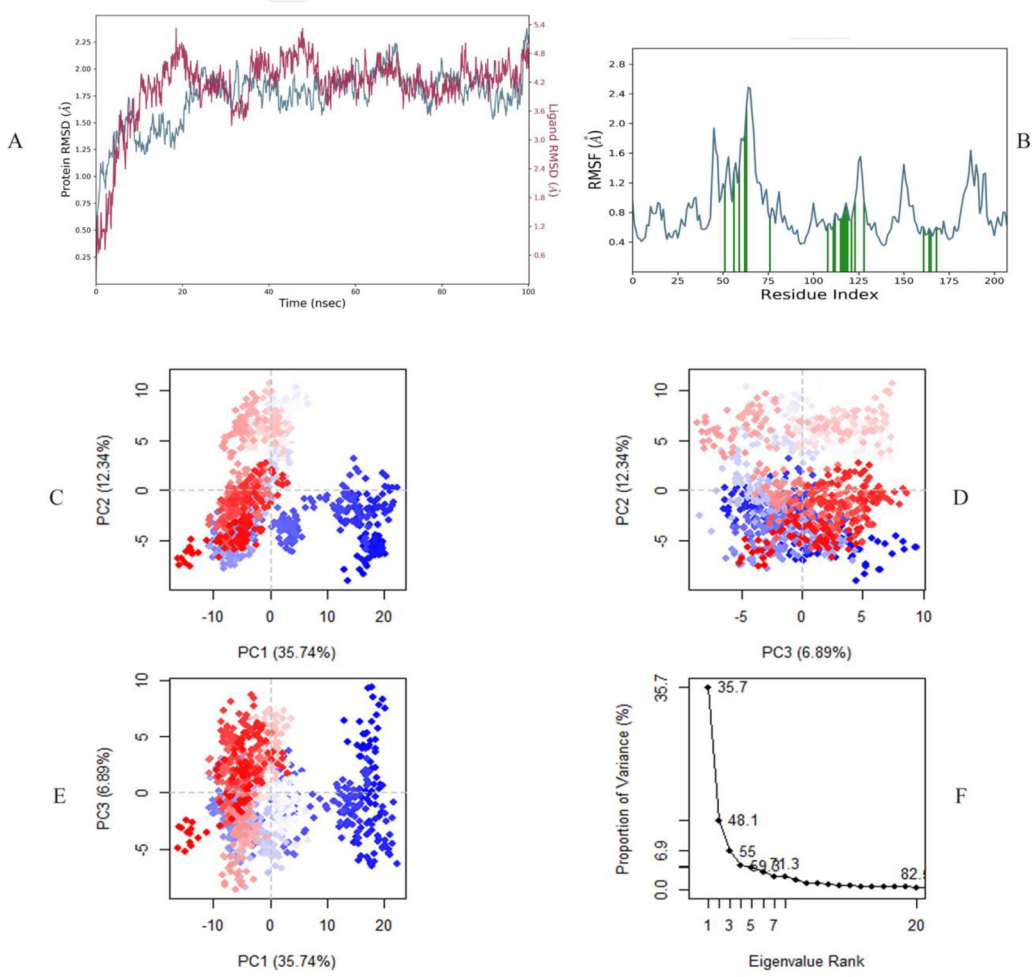

Fig. 5 **A** A 100 ns RMSD plot for simulation of azoreductase bound with CR. **B** RMSF plot of the enzyme. **C** PC1 and PC2 plot of simulation. **D** PC2 and PC3 plot of simulation. **E** PC1 and PC3 plot of simulation. **F** Eigenvalue rank plot with reference to the percent proportion of variance

to be transferred across the cell membranes. As a result, the reducing action of the dye is independent of the intracellular dye uptake. It was suggested by Russ et al. that bacterial membranes are nearly impermeable to co-factors having flavin. Therefore, they restrict reduction of sulphonated azo dyes due to equivalent transfer by cytoplasmic flavins (Russ et al. 2000). An alternate mechanism for sulphonated azoic dye reduction in cells with intact membranes occurs due to genesis of reduced flavins by the cytoplasmic flavin-dependent azoreductases (Russ et al. 2000; Feng et al. 2010; Morrison and John 2015). Another mechanism of reduction in the extra-cellular environment is based on electron transport and is achieved by establishment of link between intracellular electron transport systems of bacterial cell and azobenzene dye molecules of high molecular weight. Outer membranous electron transfer apparatus of the bacterial cell wall either makes contact directly with the azo dye substrate or interacts circuitously to the cell surface redox mediator (Sreelatha et al. 2016). Redox mediator compounds with small molecular weight have the capability to act as electron carriers among the outer membranous NADH-dependent azoreductase and azo dye (Sreelatha et al. 2016). Bacteria may synthesize redox mediators during substrate processing or these are added superficially (Russ et al. 2000). Dye reduction is hindered if the environment is aerobic as the reduced mediator is oxidized instead of azo dye. Cytoplasmic reducing enzymes supply electrons to aid redox mediators in the chemical redox process, which ultimately leads to the azo dye reduction in the cell supernatant (Xu et al. 2016; Rathod et al. 2017). This explanation seemed to fit in case of sulphonated CR dye as the degradation was reduced in aerobic conditions. Additionally, we also utilized PSORTb server for subcellular localization prediction and the enzyme was predicted to be cytoplasmic.

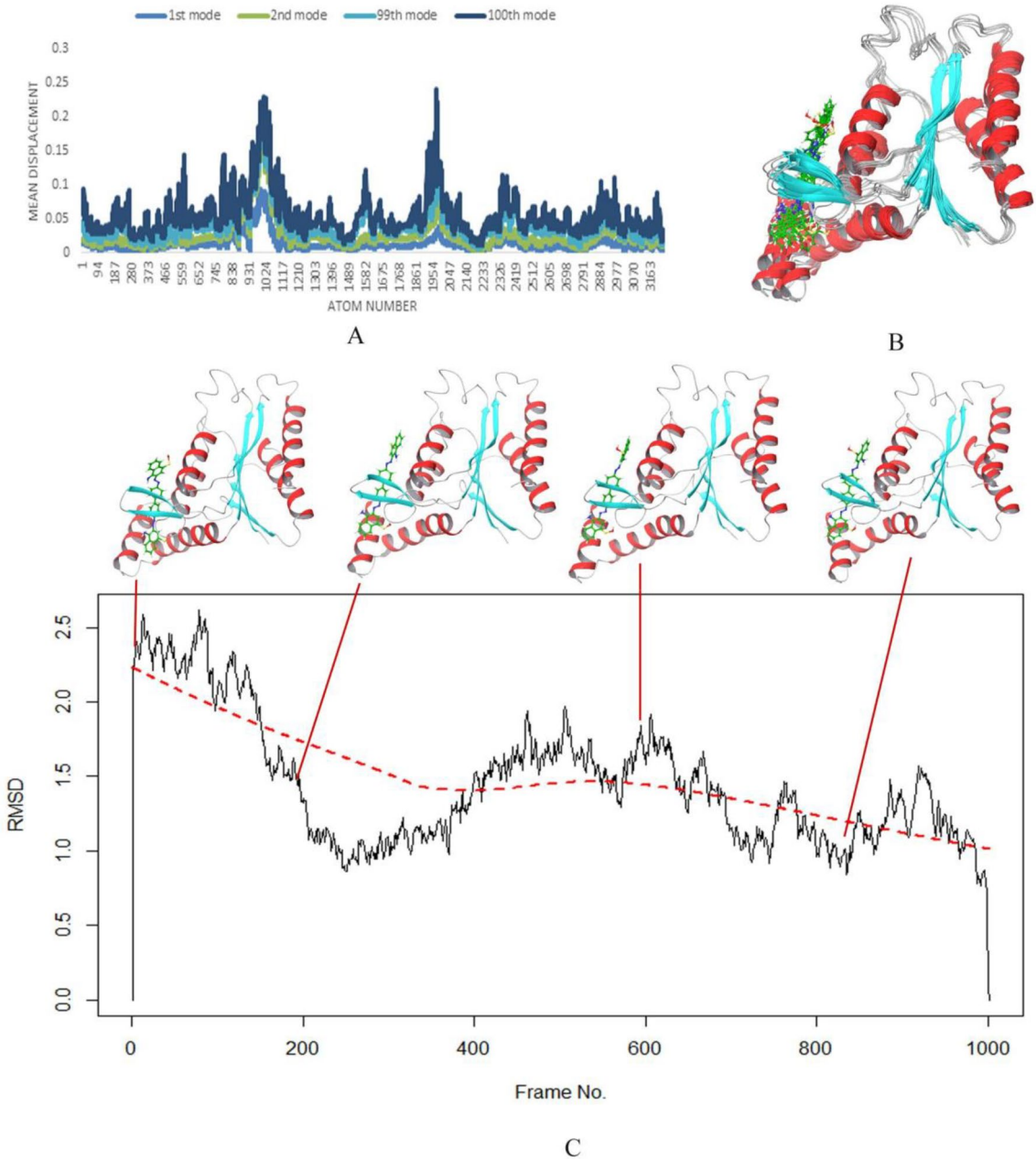

Fig. 6 **A** Comparative root-mean-square displaced plot (of C-alpha atoms) of CR bound and unbound azoreductase of *Staphylococcus caprae*. **B** Overlaid structures at 1, 20, 60, 80 and 100 ns of simulation, showing altered position of CR. **C** RMSD of frames corresponding to respective simulation time, with varied ligand position shown at first frame (1 ns of simulation), second frame (20 ns of simulation time), 600th frame (60 ns of simulation time) and 800th frame (80 ns of simulation time)

A detailed computational analysis for structure prediction, molecular docking and displaced resides after docking was conducted. Since it is time-consuming and difficult to acquire experimental structures for every protein of interest from X-ray crystallography and techniques like NMR (Wei et al. 2009), homology modelling offers handy structural models for spawning hypotheses regarding a protein's function and paving way for additional experimental work. Homology models are also helpful for deducing qualitative facets concerning the biochemistry and specific residues conservation of query sequence, and then, these hypothesized inferences can be used for experimental testing. For instance, spatially arranging conserved residues can be used for inferring if a certain arrangement stabilizes or destabilizes the folding and whether the conserved residue merely adds to the binding of a tiny molecule or promotes alliance with another nucleic acid or protein (John et al. 2011). Protein ligand docking studies can be harnessed for dye degradation

prediction by azoreductase (Patel et al. 2021) and was implemented for this study. Several studies have reported docking of azo dyes with laccase or azoreductase (Sarkar et al. 2020; Krithika et al. 2021; Mishra et al. 2023), but to the best of our knowledge, no study on *Staphylococcus* specie interaction with azoreductase exists to date. Previously, Basharat and Yasmin predicted azo dye binding with azoreductase of *Alcaligenes* sp. and found hydrogen and ionic bonds between CR and azoreductase. Both bonded and non-bonded interactions were observed for our analysis, with a Pi interaction in addition to hydrogen and ionic bonds (Basharat and Yasmin 2022). It would be interesting to explore if redox mediators are synthesized by *Staphylococcus caprae* MB400 as we did not add anything externally and MOE 2D plot showed that electron transfer seemed to occur with two residues Lys65 and Tyr124. Overall, a favourable binding was observed as MM/PBSA values of azoreductase decreased after binding to CR and this value was even lower (− 17.62) than the one obtained for *Alcaligenes faecalis* azoreductase bound with CR (− 17.52) (Basharat and Yasmin 2022).

MD simulation results complemented the docking analysis. RMSD of the azoreductase revealed good binding and trajectory analysis through PCA plotting captured motion fluctuation not exceeding 35%. This indicates that the overall motion or conformational change in the system is relatively stable, with smaller, more subtle motions or changes captured by PC2 and PC3. However, caution must be exercised when interpreting the results, as limitations in the accuracy of the force fields used in MD simulations and the approximations made during the simulation process can affect the reliability of the results. Normal mode analysis also has some limitations as it is based on the assumption that the molecule vibrates harmonically around its equilibrium conformation and is able to predict the low-frequency modes of motion that correspond to small amplitude vibrations. It cannot predict large-amplitude or anharmonic motions and does not account for solvent effects. Thus, we tried to boost our analysis by adding both techniques to study motion of atoms but limitations persist. Our study adds to the literature as no study on CR binding with *Staphylococcus* spp. exists that utilizes docking and dynamics simulation to explain the binding mechanism. Apart from giving mechanistic insights, our findings have the potential to be extended to other azoic dyes and facilitate researchers in gaining a deeper understanding of the mechanism of action of azoreductase enzymes. Additionally, this study sheds light on the substrate preference of azoreductase in *Staphylococcus caprae* and can serve as a basis for designing more effective bioremediation strategies for the removal of azo dyes from the environment. Hence, this analysis advances our knowledge on the molecular aspects on the interaction of sulphonated azo dyes with enzymes and integral role of reductases in environmental clean-up. It is hoped that this information would provide a better understanding of the molecular mechanisms, involved in catalysis and a heuristic basis for predicting the catalytic residues in related enzymes. This study could be extended for other azoic dyes and facilitate researchers in better understanding of azoreductase enzyme mechanism. The use of computational methods in studying the interaction of azo dyes with azoreductase enzymes has the potential to contribute significantly to our understanding of biodegradation processes and the development of more sustainable technologies for environmental remediation.

Conclusions

It is concluded from present study that *Staphylococcus caprae* MB400 has potential to be utilized for reduction and detoxification of CR. However, the decolourization is dependent on different factors like concentration of dye, pH and temperature of environment. This study also indicates that catalytic site made up of specific identified amino acid residues plays an important role in dye degradation through azoreductase enzyme. This information could be of importance in designing mutants and expression cloning of this azoreductase in model organisms of interest. Impact of redox co-factors like NAD and FAD could also be explored. The displacement analysis for C-alpha chain of the protein validated our findings that the most displacement was occurring in regions where residues were binding with the dye. These fluctuations are the hallmark of enzyme–substrate energy and structure change. With increasing availability of geometrical and computational methods, such analysis can be conducted in a swift manner to authenticate the interactions of enzyme binding with ligand.

Supplementary Information The online version contains supplementary material available at https://doi.org/10.1007/s00203-023-03591-z.

Author contributions AY and ZB contributed to conceptualization; ZB was involved in methodology, data curation and writing—original draft preparation, and provided software; SA and ZB contributed to validation and formal analysis; SA was involved in investigation; and AY contributed to resources, writing—review and editing, supervision and project administration. All authors have read and agreed to the published version of the manuscript.

Funding This research received no external funding.

Data availability All the data used in this manuscript is quoted as accession number or valid identifier and is within the manuscript.

Declarations

Conflict of interest The authors declare no conflict of interest.

References

Aftab U, Khan MR, Mahfooz M, Ali M, Aslam SH, Rehman A (2011) Decolourization and degradation of textile azo dyes by Corynebacterium sp. isolated from industrial effluent. Pak J Zool 43(1):1–8

Basharat Z, Yasmin A (2022) Sulphonated azo dye decolorization by Alcaligenes faecalis subsp. phenolicus MB207: insights from laboratory and computational analysis. Biophys Chem 286:106806

Basharat Z, Bibi M, Yasmin A (2017) Implications of molecular docking assay for bioremediation. Handbook of research on inventive bioremediation techniques. IGI global, pp 24–45

Basharat Z, Murtaza Z, Siddiqa A, Alnasser SM, Meshal A (2023) Therapeutic target mapping from the genome of Kingella negevensis and biophysical inhibition assessment through PNP synthase binding with traditional medicinal compounds. Mol Divers 1–14

Blümel S, Knackmuss H-J, Stolz A (2002) Molecular cloning and characterization of the gene coding for the aerobic azoreductase from *Xenophilus azovorans* KF46F. Appl Environ Microbiol 68:3948–3955

Chen K, Huang W, Wu J, Houng L (1999) Microbial decolorization of azo dyes by Proteus mirabilis. J Ind Microbiol Biotechnol 23:686–690

Cheng H-R, Jiang N (2006) Extremely rapid extraction of DNA from bacteria and yeasts. J Microbiol Biotechnol 28:55–59

d'Ersu J, Aubin G, Mercier P, Nicollet P, Bémer P, Corvec S (2016) Characterization of Staphylococcus caprae clinical isolates involved in human bone and joint infections, compared with goat mastitis isolates. J Clin Microbiol 54:106–113

Devriese* L, Poutrel B, Kilpper-Bälz R, Schleifer KH (1983) Staphylococcus gallinarum and Staphylococcus caprae, two new species from animals. Int J Syst Evol Microbiol 33:480–486

Dinçer AR (2020) Increasing BOD5/COD ratio of non-biodegradable compound (reactive black 5) with ozone and catalase enzyme combination. SN Appl Sci 2:736

Erickson K (2010) The jukes-cantor model of molecular evolution. Primus 20:438–445

Eskandari F, Shahnavaz B, Mashreghi M (2019) Optimization of complete RB-5 azo dye decolorization using novel cold-adapted and mesophilic bacterial consortia. J Environ Manag 241:91–98

Feng J, Heinze MT, Xu H, Cerniglia EC, Chen H (2010) Evidence for significantly enhancing reduction of Azo dyes in Escherichia coli by expressed cytoplasmic Azoreductase (AzoA) of Enterococcus faecalis. Protein Pept Lett 17:578–584

Fernando EY, Keshavarz T, Kyazze G (2019) The use of bioelectrochemical systems in environmental remediation of xenobiotics: a review. J Chem Technol Biotechnol 94:2070–2080

Guo G et al (2020) Azo dye decolorization by a halotolerant consortium under microaerophilic conditions. Chemosphere 244:125510

Hernández-Zamora M, Martínez-Jerónimo F (2019) Exposure to the azo dye Direct blue 15 produces toxic effects on microalgae, cladocerans, and zebrafish embryos. Ecotoxicology 28:890–902

John GSM, Rose C, Takeuchi S (2011) Understanding tools and techniques in protein structure prediction. Syst Comput Biol Bioinform Comput Model 185–212

Kanda K et al (1991) Identification of a methicillin-resistant strain of Staphylococcus caprae from a human clinical specimen. Antimicrob Agents Chemother 35:174–176

Katal R, Zare H, Rastegar SO, Mavaddat P, Darzi GN (2014) Removal of dye and chemical oxygen demand (COD) reduction from textile industrial wastewater using hybrid bioreactors. Environ Eng Manag J 13(1):43–50

Kiefer F, Arnold K, Künzli M, Bordoli L, Schwede T (2009) The SWISS-MODEL Repository and associated resources. Nucleic Acids Res 37:D387–D392

Koyani RD, Sanghvi GV, Sharma RK, Rajput KS (2013) Contribution of lignin degrading enzymes in decolourisation and degradation of reactive textile dyes. Int Biodeterior Biodegrad 77:1–9

Krithika A, Gayathri KV, Kumar DT, Doss CGP (2021) Mixed azo dyes degradation by an intracellular azoreductase enzyme from alkaliphilic Bacillus subtilis: a molecular docking study. Arch Microbiol 203:3033–3044

Kumar S, Stecher G, Li M, Knyaz C, Tamura K (2018) MEGA X: molecular evolutionary genetics analysis across computing platforms. Mol Biol Evol 35:1547

Mishra A et al (2023) Decoding whole genome of Anoxybacillus rupiensis TPH1 isolated from Tatapani hot spring, India and giving insight into bioremediation ability of TPH1 via heavy metals and azo dyes. Res Microbiol 174:104027

Morrison JM, John GH (2015) Non-classical azoreductase secretion in Clostridium perfringens in response to sulfonated azo dye exposure. Anaerobe 34:34–43

Naseer A et al (2016) Degradation and detoxification of Navy Blue CBF dye by native bacterial communities: an environmental bioremedial approach. Desalination Water Treatment 57:24070–24082

Oturkar CC, Patole MS, Gawai KR, Madamwar D (2013) Enzyme based cleavage strategy of Bacillus lentus BI377 in response to metabolism of azoic recalcitrant. Bioresour Technol 130:360–365

Pandey A, Singh P, Iyengar L (2007) Bacterial decolorization and degradation of azo dyes. Int Biodeterior Biodegrad 59:73–84

Patel GB, Rakholiya P, Shindhal T, Varjani S, Tabhani N, Shah KR (2021) Lipolytic Nocardiopsis for reduction of pollution load in textile industry effluent and SWISS model for structural study of lipase. Biores Technol 341:125673

Picho-Chillan G et al (2019) Photodegradation of Direct Blue 1 azo dye by polymeric carbon nitride irradiated with accelerated electrons. Mater Chem Phys 237:121878

Rathod J, Dhebar S, Archana G (2017) Efficient approach to enhance whole cell azo dye decolorization by heterologous overexpression of Enterococcus sp. L2 azoreductase (azoA) and Mycobacterium vaccae formate dehydrogenase (fdh) in different bacterial systems. Int Biodeterior Biodegrad 124:91–100

Russ R, Rau J, Stolz A (2000) The function of cytoplasmic flavin reductases in the reduction of azo dyes by bacteria. Appl Environ Microbiol 66:1429–1434

Saratale RG et al (2013) Decolorization and detoxification of sulfonated azo dye CI Remazol Red and textile effluent by isolated Lysinibacillus sp RGS. J Biosci Bioeng 115:658–667

Sarkar S, Banerjee A, Halder U, Biswas R, Bandopadhyay R (2017) Degradation of synthetic azo dyes of textile industry: a sustainable approach using microbial enzymes. Water Conserv Sci Eng 2:121–131

Sarkar S, Banerjee A, Chakraborty N, Soren K, Chakraborty P, Bandopadhyay R (2020) Structural-functional analyses of textile dye degrading azoreductase, laccase and peroxidase: a comparative in silico study. Electron J Biotechnol 43:48–54

Shah MP (2019) Bioremediation of azo dye. Microbial wastewater treatment. Elsevier, pp 103–126

Singh K, Arora S (2011) Removal of synthetic textile dyes from wastewaters: a critical review on present treatment technologies. Crit Rev Environ Sci Technol 41:807–878

Sreelatha S, Velvizhi G, Kumar AN, Mohan SV (2016) Functional behavior of bio-electrochemical treatment system with increasing azo dye concentrations: Synergistic interactions of biocatalyst and electrode assembly. Bioresour Technol 213:11–20

Srinivasan S, Sadasivam SK (2018) Exploring docking and aerobic-microaerophilic biodegradation of textile azo dye by bacterial systems. J Water Process Eng 22:180–191

Suhre K, Sanejouand Y-H (2004) ElNemo: a normal mode web server for protein movement analysis and the generation of templates for molecular replacement. Nucleic Acids Res 32:W610–W614

Suzuki Y, Yoda T, Ruhul A, Sugiura WJ (2001) Molecular cloning and characterization of the gene coding for azoreductase from Bacillus sp. OY1–2 isolated from soil. J Biol Chem 276:9059–9065

Vandenesch F, Eykyn SJ, Bes M, Meugnier H, Fleurette J, Etienne J (1995) Identification and ribotypes of Staphylococcus caprae isolates isolated as human pathogens and from goat milk. J Clin Microbiol 33:888–892

Wei T, Gong J, Jamitzky F, Heckl WM, Stark RW, Rössle SC (2009) Homology modeling of human Toll-like receptors TLR7, 8, and 9 ligand-binding domains. Protein Sci 18:1684–1691

Wilson K (1987) Preparation of genomic DNA from bacteria. Curr Protocols Mol Biol 241–245

Xu F, Mou Z, Geng J, Zhang X, Li C-Z (2016) Azo dye decolorization by a halotolerant exoelectrogenic decolorizer isolated from marine sediment. Chemosphere 158:30–36

Yadav A, Mukherji S, Garg A (2013) Removal of chemical oxygen demand and color from simulated textile wastewater using a combination of chemical/physicochemical processes. Ind Research Eng Chem Res. 52:10063–10071

Yagub MT, Sen TK, Afroze S, Ang HM (2014) Dye and its removal from aqueous solution by adsorption: a review. Adv Colloid Interface Sci 209:172–184

Yang H et al (2019) admetSAR 2.0: web-service for prediction and optimization of chemical ADMET properties. Bioinformatics 35:1067–1069

Yu NY et al (2010) PSORTb 3.0: improved protein subcellular localization prediction with refined localization subcategories and predictive capabilities for all prokaryotes. Bioinformatics 26:1608–1615